# Atomic layer deposition for hafnium oxide-based meta-optics in the ultraviolet spectral range

*Thomas Siefke*[*,1,2,3], *Kristin Gerold*[1,2], *Svetlana Shestaeva*[2], *Pallabi Paul*[1,2], *Shawon Alam*[4], *Daniel Franta*[5], *Adriana Szeghalmi*[1,2], *Sven Schröder*[2] *and Stefanie Kroker*[6,7,8]

[1]Friedrich-Schiller-University, Institute of Applied Physics, Albert-Einstein-Strasse 15, 07745 Jena, Germany
[2]Fraunhofer Institute for Applied Optics and Precision Engineering IOF, Albert-Einstein-Str. 7, 07745 Jena, Germany
[3]Ernst-Abbe-Hochschule Jena, University of Applied Sciences, Carl-Zeiss-Promenade 2, 07745 Jena, Germany
[4]Karlsruhe Institute of Technology (KIT), Kaiserstraße 12, 76131 Karlsruhe
[5]Department of Plasma Physics and Technology, Faculty of Science, Masaryk University, Kotlářská 2, 61137 Brno, Czechia
[6]TU Braunschweig, Institute of Semiconductor Technology, Hans-Sommer-Str. 66, 38106 Braunschweig, Germany
[7]TU Braunschweig, LENA Laboratory for Emerging Nanometrology, Langer Kamp 6a/b, 38106 Braunschweig, Germany
[8]Physikalisch-Technische Bundesanstalt, Bundesallee 100, 38116 Braunschweig, Germany

**Abstract.** Hafnium oxide ($HfO_2$) is a high-index dielectric material of growing importance for optical coatings and meta-optical components operating from the ultraviolet (UV) to the visible spectral range. Its large bandgap, chemical stability, and compatibility with established semiconductor processes make it particularly attractive for applications requiring low absorption and precise thickness control. In this work, we investigate the optical material properties of $HfO_2$ thin films deposited by plasma-enhanced atomic layer deposition (PEALD). The complex refractive index is experimentally determined over a broad spectral range extending from the vacuum ultraviolet (140 nm) to the visible (600 nm) by combining spectroscopic ellipsometry, spectrophotometry, and infrared ellipsometry. A comprehensive dispersion model is employed to extract consistent optical constants and thickness values. The results highlight the suitability of PEALD-grown $HfO_2$ films for advanced optical and meta-optical applications.

**Keywords:** Hafniumoxide, meta-optics, ultra violet, refractive index, atomic layer deposition.

## 1 Introduction

Hafnium oxide ($HfO_2$) has attracted significant attention over the past two decades as a functional material in both microelectronics and photonics. In microelectronic devices, $HfO_2$ is well established as a high-permittivity (high-k) dielectric replacing $SiO_2$ in advanced

* Corresponding author: thomas.siefke@uni-jena.de

This provisional PDF is the accepted version. The article should be cited as: J. Eur. Opt. Society-Rapid Publ., https://doi.org/10.1051/jeos/2026036

metal–oxide–semiconductor field-effect transistors [1-3].Beyond its electronic functionality, the optical properties of $HfO_2$, namely its high refractive index, wide optical bandgap, and high transparency from the ultraviolet to the infrared, render it attractive for optical coatings, interference filters, and dielectric metasurfaces [4-7]. In particular, the demand for optical components such as wire grid polarizer [8,9], meta lenses [10] or diffractive optical elements [11] or grating couplers in photonic integrated circuits [12] operating in the ultraviolet and vacuum ultraviolet spectral ranges has increased substantially due to applications in spectroscopy - especially in quantum technologies [13-15] - space optics, and high-resolution microscopy. For these applications, materials must combine low optical absorption with high refractive index contrast and excellent environmental stability. $HfO_2$ fulfills these requirements and offers superior laser-induced damage threshold (LIDT) [16,17] as well as resistance to radiation-induced damage [18,19] and chemical degradation and corrosion compared to many alternative high-index oxides. A large variety of deposition techniques have been employed for $HfO_2$ thin films, such as electron beam evaporation [20, 21], magnetron sputtering [22], ion beam sputtering [23,24], sol-gel [25-27] and atomic layer deposition (ALD) [28-33]. Among these, ALD is particularly suitable for the fabrication of $HfO_2$ thin films with precisely controlled thickness and excellent structural conformality. The self-limiting surface reactions inherent to ALD enables uniform coatings on both planar as well as three-dimensional nanostructured substrates, which is essential for emerging meta-optical concepts relying on subwavelength structuring.

Numerous studies have been reported on the optical and structural properties of ALD-grown $HfO_2$, demonstrating its applicability in optical thin films across a wide spectra range, for instance as anti-reflection coatings at 266 nm, 355 nm, 532 nm and/or 1064 nm [31,33], or as high-reflective mirrors at 355 nm and 532 nm [32]. Nevertheless, comprehensive experimental data on its optical constants over an extended spectral range, particularly toward the vacuum ultraviolet (VUV) remain comparatively scarce.

The present work aims to expand the accessible optical database by providing detailed optical properties of PEALD $HfO_2$ thin films down to a wavelength of 140 nm. By combining multiple complementary measurement techniques [34,35], we extract reliable optical constants from the visible to the VUV range. The resulting dataset provides a solid foundation for the optical design and simulation of $HfO_2$-based coatings and meta-optical devices.

## 2. Thin film deposition

Hafnium oxide thin films are commonly deposited by atomic layer deposition using a variety of hafnium precursor chemistries in combination with either thermal or plasma-assisted oxidation steps. In thermal ALD, both inorganic precursors such as hafnium tetrachloride ($HfCl_4$) [36] and metal–organic precursors tetrakis(dimethylamido)hafnium (TDMAH), tetrakis(ethylmethylamido)hafnium (TEMAH) [37], or β-diketonate-based [38, 39] compounds have been widely employed together with water as the oxidant. While $HfCl_4$-based processes typically require higher deposition temperatures and may lead to halogen-related impurities, metal–organic precursors enable lower-temperature growth and improved process flexibility. In plasma-enhanced ALD (PEALD), the molecular oxidant is replaced by an oxygen plasma, which enhances ligand removal and film densification [40]. PEALD processes using TDMAH or TEMAH have been shown to produce dense, stoichiometric $HfO_2$ films with reduced impurity content at comparatively low substrate temperatures [30-32], making them especially attractive for optical coatings and nanophotonic applications.

Depending on the chosen precursor chemistry and oxidation scheme, the resulting films may exhibit significant differences in growth per cycle, density, impurity concentration, and ultimately optical material properties. The $HfO_2$ thin films investigated in this study were

deposited at 100°C using plasma-enhanced atomic layer deposition in an OpAL reactor (Oxford Instruments Plasma Technology). Tetrakis(dimethylamido)hafnium (TDMAH, $Hf[N(CH_3)_2]_4$) served as the metal precursor, while an oxygen plasma was employed as the oxidizing reactant. Each ALD cycle consisted of a TDMAH precursor pulse (0.4 s), followed by a purge (8 s) and pump-down (2 s) sequence to remove excess precursor and by-products, a gas stabilization period (3 s) followed by an oxygen plasma exposure (10 s) and a final purge (10 s). The details are summarized in Table 1.

The deposition was performed on fused silica substrates in order to enable transmission measurements over a wide spectral range. To ensure sufficient optical sensitivity in ellipsometry measurements while maintaining negligible interference from the substrate backside, a total film thickness of approximately 200 nm was targeted. The deposition process yielded smooth, homogeneous films with excellent macroscopic uniformity.

*Table 1: ALD parameter for Hafnia deposition using TDMAH and oxygen plasma in an OPAL-tool.*

| Step | Parameter | Value |
|---|---|---|
| 1 | TDMAH pulse time | 0.4 s |
| 2 | Purge time | 8 s |
| 3 | Pump down time | 2 s |
| 4 | Gas stabilization time | 3 s |
| 5 | Oxygen plasma pulse | |
| | Time | 10s |
| | Flow | 50 sccm |
| | Power | 300 W |
| 6 | Purge time | 10 s |

## 3. Optical characterization methods

The optical properties of the $HfO_2$ films were characterized using a combination of spectroscopic ellipsometry and spectrophotometry to cover a broad spectral range. Vacuum ultraviolet and ultraviolet ellipsometric measurements were performed using a Jobin Yvon UVISEL2 ellipsometer at photon energies ranging from 1.5 to 8.7 eV at a fixed angle of incidence of 70°. Additional ellipsometric data in the range from 0.6 to 6.5 eV were acquired with a Jobin Yvon UVISEL ellipsometer using multiple angles of incidence between 55° and 75°. Infrared ellipsometry measurements covering the range from 300 to 6500 $cm^{-1}$ were conducted using a Woollam IR-VASE ellipsometer, again employing variable angles of incidence. Complementary transmission and reflection spectra were recorded using a Perkin Elmer Lambda 1050 spectrophotometer and a Bruker Vertex 80v Fourier-transform infrared spectrometer. For reflectance measurements, illumination from both the film and substrate side was used to enhance sensitivity to interface effects. The experimental data were analyzed using the universal dispersion model implemented in the newAD2 software package [34]. All relevant parameters, including film thickness, dispersion coefficients, and interface roughness, were treated as free fitting parameters. This approach ensured a consistent description of the optical response across all spectral regions and measurement techniques.

125 ## 4. Results and discussion

126

127 The combined optical analysis yielded film thickness values between 217 and 221 nm,
128 depending on the specific measurement configuration and spot size. This small variation
129 indicates a high degree of thickness uniformity across the sample. The surface roughness of
130 the top interface was determined to be approximately 1.51 nm (root mean square), with an
131 autocorrelation length of about 5.3 nm. These values correspond to dense, smooth oxide
132 layers produced with PEALD and are comparable to $HfO_2$ thin films on silicon reference
133 samples deposited under similar conditions with 0.8 nm rms (XRR) [29]. The low surface
134 roughness is critical for optical applications, as elevated topography would introduce scatter
135 losses and degrade coating performance in the ultraviolet spectral range.
136 To evaluate film quality and optical functionality, the extracted refractive index was
137 compared with a previous PEALD-$HfO_2$ study. The thin film examined in this work is
138 designated Type A, while the comparison sample is designated Type B (compare Fig. 1 and
139 Table 2). To minimize the influence of impurity contributions on the optical properties, we
140 compare only processes performed with the same precursor (TDMAH) same oxidizing agent
141 ($O_2$-plasma) and at the same deposition temperature (100 °C), since these are the main
142 parameters affecting carbon and nitrogen levels [30]. The low deposition temperature was
143 chosen to reduce crystallization in the thin films, even though lower temperatures often lead
144 to increased carbon contamination because of incomplete precursor oxidation.
145 The refractive index of both $HfO_2$ thin films exhibits a pronounced wavelength
146 dependence, with a normal dispersion i.e. high values in the visible and near-ultraviolet
147 spectral range and a gradual decrease toward longer wavelengths. In the ultraviolet region,
148 the refractive index increases significantly as the photon energy approaches the optical band
149 edge, while absorption remains negligible over a wide spectral range down to 230 nm
150 (compare band edge of 5.6 eV [33]). This behaviour is highly advantageous for optical
151 coatings and metasurfaces requiring strong phase modulation with minimal optical losses.
152 While both $HfO_2$ thin films demonstrate excellent optical properties and comparable
153 transparent regions, Type A and Type B show slight deviations in refractive index. These
154 differences can be attributed to two distinct sources: differences in metrology and deposition
155 conditions.
156 For Type A thin films, the universal dispersion model (UDM) was employed to extract
157 optical constants [34]. In contrast, optical constants of Type B thin films were extracted from
158 VUV transmittance and reflectance spectra using the Lorentz Calculator (LCalc) [41]. These
159 different analytical methods can introduce systematic deviation, particularly in the VUV
160 region where extinction is dominated by complex inter-band transitions. Nevertheless, both
161 methods are sufficiently mature to provide reliable data and inherently capture the material
162 response, including any influence of i.e. residual impurities.
163 Typically, different deposition parameters are the main source of such differences. The
164 dominant factor separating the two film types are the different PEALD reactor configuration
165 and associated plasma parameters, which are known to strongly influence $HfO_2$ film density
166 and refractive index [31]. Type A films were deposited using an OpAL PEALD reactor with
167 a remote Inductively Coupled Plasma (ICP) source, while Type B samples were produced on
168 a SILAYO-ICP330 system (Sentech Instruments GmbH), equipped with a direct ICP
169 configuration featuring a Planar Triple Spiral Antenna (PTSA) source. These distinct plasma
170 architectures lead to markedly different energy input and ion bombardment characteristics.
171 The SILAYO PTSA-ICP source delivers higher plasma power density and enhanced ion flux,
172 enabling more effective energetic assistance during film growth. This results in denser films:
173 Type B achieves 8.25 $g/cm^3$ compared to 7.90 $g/cm^3$ for Type A (Table 2). Film density is
174 directly reflected in the refractive index; the denser Type B films exhibit higher n-values

175 across the transparent spectral range. This density-dependent optical property improvement
176 is a well-established phenomenon in oxide thin films and confirms that plasma parameter
177 optimization is a critical control lever for tailoring optical performance in PEALD-$HfO_2$
178 systems.

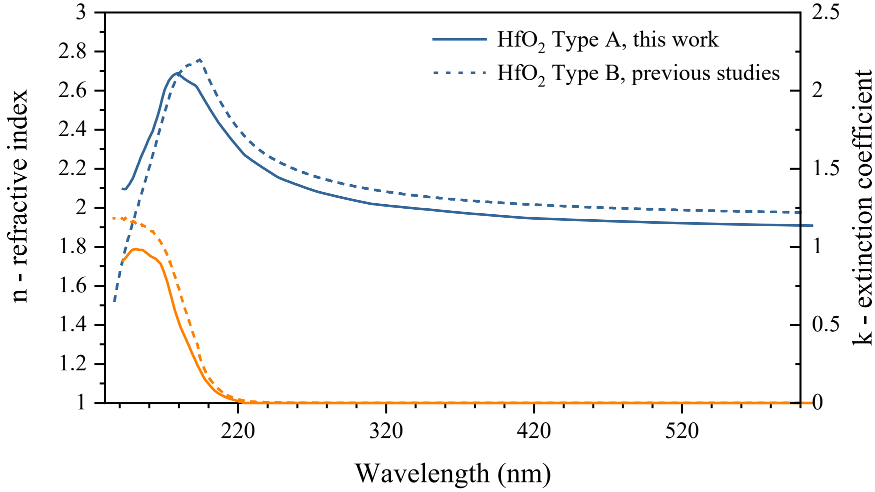


179
180
181 **Fig. 1.** Wavelength dependence of the refractive index of the fabricated hafnia thin films.
182
183
184 *Table 2: Compared HfO2 thins films prepared by PEALD with different ALD tools.*

| | $HfO_2$ – Type A | $HfO_2$ – Type B |
|---|---|---|
| **reference** | this work; [29] | [33] |
| **PEALD tool** | OpAL | SILAYO-ICP330 |
| **precursors** | TDMAH + $O_2$ plasma | TDMAH + $O_2$ plasma |
| **substrate temperature** | 100°C | 100°C |
| **density** | 7.90 gcm-3 | 8.25 gcm-3 |
| **surface roughness** | 0.8 nm (XRR) | 1.07 nm (AFM) |

185
186 X-ray diffraction measurements conducted at the deposition temperature (100 °C)
187 indicate that both Type A and Type B films are X-ray amorphous (not shown here), consistent
188 with low-temperature PEALD processes. However, X-ray amorphous coatings can contain
189 nanocrystalline domains, short-range crystalline order, or point defects that influence optical
190 properties. This may also explain the moderate deviations, especially observed below the
191 absorption edge between the two film sets. The higher density of type B can encourage slight
192 structural rearrangement, such as localized crystallization or structural densification, and
193 affect the absorption profile below the band gap. Despite these structural subtleties, both
194 films maintain low absorption in the transparent region and preserve well-defined optical
195 bandgaps, indicating that any nanocrystalline or defect-state contributions remain minimal
196 and do not compromise optical performance.
197 The results of both $HfO_2$ thin films conclusively confirm that PEALD enables the
198 fabrication of optically dense $HfO_2$ layers with properties suitable for advanced optical
199 designs, including applications in ultraviolet meta-optics.

## 5. Conclusion

In summary, we have presented a comprehensive optical characterization of hafnium oxide thin films deposited by plasma-enhanced atomic layer deposition. By combining spectroscopic ellipsometry and spectrophotometry across a wide spectral range, reliable optical constants from the infrared to the vacuum ultraviolet were obtained. The films exhibit high refractive indices, low surface roughness, and excellent optical homogeneity. These findings underscore the suitability of ALD-grown $HfO_2$ for demanding optical applications, particularly in the ultraviolet spectral range and in nanostructured meta-optical systems. The presented dataset provides a valuable reference for optical modeling and design and supports the further development of $HfO_2$-based optical components.


## 2 Funding

The research has been supported by the Deutsche Forschungsgemeinschaft (DFG) (Emmy-Noether-Project SZ253/1-1, 287542364 and Collaborative Research Center (CRC/SFB) 1375), the European Space Agency (ESA) (Contract No. 4000109161/13/NL/RA), under Grant No. 13N16897 GRADIENT, and BMFTR, Förderprogramm Fusion2040 – Forschung auf dem Weg zum Fusionskraftwerk, FKZ: 13F1009I, SHARP and ATIQ (Fkz: 13N16116), Cluster of excellence QuantumFrontiers (ExC-2123-390837967) as well as from the EMPIR programme 20IND04 ATMOC.


## 3 Conflict of interests

The authors declare that they have no competing interests to report.

## 4 Data availability statement

The data that support the findings of this study will be made publicly available in the refractiveindex.info database (https://refractiveindex.info/) upon publication.

## 5 Author contribution statement

Thomas Siefke contributed to writing (original draft), formal analysis, funding acquisition, and resources. Kristin Gerold contributed to writing (original draft), visualization, formal analysis, and investigation. Svetlana Shestaeva contributed to writing (review and editing), formal analysis, and investigation. Pallabi Paul contributed to formal analysis, and investigation. Shawon Alam contributed to formal analysis, and investigation. Daniel Franta contributed to formal analysis and investigation. Adriana Szeghalmi contributed to funding acquisition and writing (review and editing). Sven Schröder contributed to writing (review and editing). Stefanie Kroker contributed to funding acquisition and writing (review and editing).

239 ## References


240 1. Yin YT, Huang CC, Chiu PH, Jiang Y Sen, Hoo JY, Chen MJ. High-Quality HfO2
241 High-K Gate Dielectrics Deposited on Highly Oriented Pyrolytic Graphite via
242 Enhanced Precursor Atomic Layer Seeding. ACS Appl Electron Mater 7:1943–52
243 (2025). https://doi.org/10.1021/ACSAELM.4C02224

244 2. Zhang S, Zhang T, Yu H, Li T, Li X, Cui C, et al. Wafer-scale high-κ HfO2 dielectric
245 films with sub-5-Å equivalent oxide thickness for 2D MoS2 transistors. Nat Commun
246 17, 1888 (2026). https://doi.org/10.1038/s41467-026-68584-0

247 3. Choi JH, Mao Y, Chang JP. Development of hafnium based high-k materials—A
248 review. Mater Sci Eng R Rep 72:97–136(2011).
249 https://doi.org/10.1016/J.MSER.2010.12.001.

250 4. Chow R, Falabella S, Loomis GE, Rainer F, Stolz CJ, Kozlowski MR. Reactive
251 evaporation of low-defect density hafnia. Appl Opt 32, 5567(1993).
252 https://doi.org/10.1364/AO.32.005567.

253 5. Lehan JP, Mao Y, Bovard BG, Macleod HA. Optical and microstructural properties of
254 hafnium dioxide thin films. Thin Solid Films 203:227–50 (1991).
255 https://doi.org/10.1016/0040-6090(91)90131-G.

256 6. Balog M, Schieber M, Michman M, Patai S. Chemical vapor deposition and
257 characterization of HfO2 films from organo-hafnium compounds. Thin Solid Films
258 41:247–59(1977). https://doi.org/10.1016/0040-6090(77)90312-1.

259 7. Ritala M, Leskelä M, Niinistö L, Prohaska T, Friedbacher G, Grasserbauer M.
260 Development of crystallinity and morphology in hafnium dioxide thin films grown by
261 atomic layer epitaxy. Thin Solid Films 250:72–80(1994). https://doi.org/10.1016/0040-
262 6090(94)90168-6

263 8. Stock C, Siefke T, Zeitner U. Metasurface-based patterned wave plates for VIS
264 applications. J Opt Soc Am B36:D97 (2019).
265 https://doi.org/10.1364/JOSAB.36.000D97

266 9. Siefke T, Kley E-B, Tünnermann A, Kroker S. Design and fabrication of titanium
267 dioxide wire grid polarizer for the far ultraviolet spectral range. In: Campo EM, Dobisz
268 EA, Eldada LA, editors. Proceedings of SPIE - The International Society for Optical
269 Engineering, vol. 9927 (2016). https://doi.org/10.1117/12.2237644.

270 10. Ossiander M, Meretska ML, Hampel HK, Lim SWD, Knefz N, Jauk T, et al. Extreme
271 ultraviolet metalens by vacuum guiding. Science 1979, 380:59–63(2023).
272 https://doi.org/10.1126/SCIENCE.ADG6881

273 11. Kaufmann J, Siefke T, Ronning C, Zeitner UD. Fabrication of EUV Gratings via Ion
274 Irradiation JW4A.15 (2024).

275 12. Sorokina A, Meyer AA, Grimpe CF, Du G, Sauer S, Jordan JE, Mehlstäubler TE,
276 Kroker S, Numerical analysis of a high-efficiency dual-material waveguide-grating
277 coupler system for ultraviolet photonics. Opt Continuum 4, 10, (2025).
278 https://doi.org/10.1364/OPTCON.568352.

279 13. Alombert-Goget G, Trichard F, Li H, Pezzani C, Silvestre M, Barthalay N, et al.
280 Titanium distribution profiles obtained by luminescence and LIBS measurements on
281 Ti: Al2O3 grown by Czochralski and Kyropoulos techniques. Opt Mater
282 (Amst);65:28–32 (2017). https://doi.org/10.1016/J.OPTMAT.2016.09.049.

283 14. Trichard F, Moncayo S, Devismes D, Pelascini F, Maurelli J, Feugier A, et al.
284 Evaluation of a compact VUV spectrometer for elemental imaging by laser-induced

285 breakdown spectroscopy: application to mine core characterization. J Anal At
286 Spectrom 32:1527–34(2017). https://doi.org/10.1039/C7JA00185A.

287 15. Bassel L, Motto-Ros V, Trichard F, Pelascini F, Ammari F, Chapoulie R, et al. Laser-
288 induced breakdown spectroscopy for elemental characterization of calcitic alterations
289 on cave walls. Environ Sci Pollut Res 24:2197–204 (2017).
290 https://doi.org/10.1007/S11356-016-7468-5/FIGURES/5.

291 16. Alvisi M, Di Giulio M, Marrone SG, Perrone MR, Protopapa ML, Valentini A, et al.
292 HfO2 films with high laser damage threshold. Thin Solid Films 358:250–8(2000).
293 https://doi.org/10.1016/S0040-6090(99)00690-2.

294 17. Stolz CJ, Thomas MD, Griffin AJ. BDS thin film damage competition. 7132:107–
295 13(2008). https://doi.org/10.1117/12.806287.

296 18. Fan Y, Liu J, Jiang J, Jiang LM. Ion Radiation Effects on the Stability of Hafnium
297 Oxide-Based Ferroelectric Thin Films: Mechanisms and Regulation. IEEE Trans
298 Device Mater Rel 25:314–22 (2025). https://doi.org/10.1109/TDMR.2025.3550950.

299 19. Ding M, Liu X. Damage effect of hafnium oxide gate dielectric based metal-oxide-
300 semiconductor structure under gamma-ray irradiation. AIP Adv 11:65304 (2021).
301 https://doi.org/10.1063/5.0048080/993914.

302 20. Kant S, Kumari N, Kumar M. Effect of deposition conditions on the morphological,
303 optical, and corrosion behavior of electron beam evaporated high-performance HfO2
304 thin films. Appl Phys A 131, 631 (2025). https://doi.org/10.1007/s00339-025-08755-w

305 21. Ramzan M, Rana AM, Ahmed E, Bhatti AS, Hafeez M, Ali A, et al. Optical
306 description of HfO2/Al/HfO2 multilayer thin film devices. Curr Appl Phys 14:1854–60
307 (2014). https://doi.org/10.1016/J.CAP.2014.10.023.

308 22. Araiza J de J, Álvarez-Fraga L, Gago R, Sánchez O. Surface Morphology and Optical
309 Properties of Hafnium Oxide Thin Films Produced by Magnetron Sputtering. Materials
310 16, 5331 (2023) https://doi.org/10.3390/MA16155331.

311 23. Thielsch R, Gatto A, Kaiser N. Mechanical stress and thermal-elastic properties of
312 oxide coatings for use in the deep-ultraviolet spectral region. Appl Opt 41, 16 (2002)
313 https://doi.org/10.1364/AO.41.003211.

314 24. Bundesmann C, Neumann H. Tutorial: The systematics of ion beam sputtering for
315 deposition of thin films with tailored properties. J Appl Phys 124:231102(2018).
316 https://doi.org/10.1063/1.5054046.

317 25. Jiang K, Anderson JT, Hoshino K, Li D, Wager JF, Keszler DA. Low-Energy Path to
318 Dense HfO2 Thin Films with Aqueous Precursor. Chem Mater 23 (4), 945-952 (2011).
319 https://doi.org//10.1021/cm102082j.

320 26. Nishide T, Honda S, Matsuura M, Ide M. Surface, structural and optical properties of
321 sol-gel derived HfO2 films. Thin Solid Films 371, 61 (2000)
322 https://doi.org/10.1016/S0040-6090(00)01010-5.

323 27. Zaharescu M, Teodorescu VS, Gartner M, Blanchin, MG, Barau A, Anastasescu M.
324 Correlation between the method of preparation and the properties of the sol–gel HfO2
325 thin films. J Non-Cryst Solids, 354, 409 (2008)
326 https://doi.org/10.1016/j.jnoncrysol.2007.07.097.

327 28. Kull M, Piirsoo HM, Tarre A, Mändar H, Tamm A, Jõgiaas T. Hardness, Modulus, and
328 Refractive Index of Plasma-Assisted Atomic-Layer-Deposited Hafnium Oxide Thin
329 Films Doped with Aluminum Oxide. Nanomaterials 13:1607(2023).
330 https://doi.org/10.3390/NANO13101607/S1.

331 29. Shestaeva S, Bingel A, Munzert P, Ghazaryan L, Patzig P, Tünnermann A, Szeghalmi
332 A. Mechanical, structural, and optical properties of PEALD metallic oxides for optical
333 applications. Appl Opt 56, 4 (2017) https://doi.org/10.1364/AO.56.000C47.
334 30. Kim K-M, Jang JS, Yoon S-G, Yun J-Y, Chung N-K. Structural, Optical and Electrical
335 Properties of $HfO_2$ Thin Films Deposited at Low-Temperature Using Plasma-Enhanced
336 Atomic Layer Deposition. Materials 13(9), 2008 (2020).
337 https://doi.org/10.3390/ma13092008
338 31. Lapteva M, Beladiya V, Riese S, Hanke P, Otto F, Fritz T, Schmitt P, Olaf Stenzel O,
339 Andreas Tünnermann A, Szeghalmi A. Influence of temperature and plasma
340 parameters on the properties of PEALD $HfO_2$, Opt Mater Express 11, 1918-
341 1942(2021). https://doi.org/10.1364/OME.422156
342 32. Beladiya V, Faraz T, Schmitt P, Munser AS, Schröder S, Riese S, Mühlig C,
343 Schachtler D, Steger F, Botha R, Otto F, Fritz T, Helvoirt C, Kessels WMM, Gargouri
344 H, Szeghalmi A, Plasma-Enhanced Atomic Layer Deposition of $HfO_2$ with Substrate
345 Biasing: Thin Films for High-Reflective Mirrors, ACS Appl Mater Interfaces 14,
346 14677−14692 (2022). https://doi.org/10.1021/acsami.1c21889
347 33. Alam S, Paul P, Beladiya V, Schmitt P, Stenzel O, Trost M, Wilbrandt S, Mühlig C,
348 Schröder S, Matthäus G, et al. Heterostructure Films of $SiO_2$ and $HfO_2$ for High-Power
349 Laser Optics Prepared by Plasma-Enhanced Atomic Layer Deposition. Coatings 13,
350 278 (2023). https://doi.org/10.3390/coatings13020278
351 34. Franta D, Nečas D, Ohlídal I. Universal dispersion model for characterization of
352 optical thin films over a wide spectral range: application to hafnia. Appl Opt 54:9108
353 (2015). https://doi.org/10.1364/AO.54.009108.
354 35. Siefke T, Kroker S, Pfeiffer K, Puffky O, Dietrich K, Franta D, et al. Materials Pushing
355 the Application Limits of Wire Grid Polarizers further into the Deep Ultraviolet
356 Spectral Range. Adv Opt Mater 4:1780–6(2016).
357 https://doi.org/10.1002/adom.201600250.
358 36. Puurunen RL, Appl Phys J, Vac Sci Technol JA. Analysis of hydroxyl group controlled
359 atomic layer deposition of hafnium dioxide from hafnium tetrachloride and water. J
360 Appl Phys 95:4777–86(2004). https://doi.org/10.1063/1.1689732.
361 37. Triyoso DH, Hegde RI, White BE, Tobin PJ. Physical and electrical characteristics of
362 atomic-layer-deposited hafnium dioxide formed using hafnium tetrachloride and
363 tetrakis(ethylmethylaminohafnium). J Appl Phys 97:124107(2005).
364 https://doi.org/10.1063/1.1947389
365 38. Pasko S V., Hubert-Pfalzgraf LG, Abrutis A, Richard P, Bartasyte A, Kazlauskiene V.
366 New sterically hindered Hf, Zr and Y β-diketonates as MOCVD precursors for oxide
367 films. J Mater Chem 14:1245–51(2004). https://doi.org/10.1039/B401052C.
368 39. Zherikova K V., Morozova NB, Zelenina LN, Sysoev S V., Chusova TP, Igumenov
369 IK. Thermal properties of hafnium(IV) and zirconium(IV) β-diketonates. J Therm Anal
370 Calorim 92, 729–34(2008). https://doi.org/10.1007/s10973-008-9027-x.
371 40. Martínez-Puente MA, Horley P, Aguirre-Tostado FS, López-Medina J, Borbón-Nuñez
372 HA, Tiznado H, et al. ALD and PEALD deposition of HfO2 and its effects on the
373 nature of oxygen vacancies. Mater Sci Eng B 285, 115964 (2022).
374 https://doi.org/10.1016/J.MSEB.2022.115964.
375 41. Stenzel, O.; Wilbrandt, S.; Friedrich, K.F.; Kaiser, N. Realistische Modellierung der
376 NIR/VIS/UV-optischen Konstanten dünner optischer Schichten im Rahmen des
377 Oszillatormodells. VIP 21, 15–23(2009). https://doi.org/10.1002/vipr.200900396